

# Humanization of Chicken-Derived scFv Using Yeast Surface Display and NGS Data Mining

Adrian Elter, Jan P. Bogen, Steffen C. Hinz, David Fiebig, Arturo Macarrón Palacios, Julius Grzeschik, Björn Hock, and Harald Kolmar\*

Generation of high-affinity monoclonal antibodies by immunization of chickens is a valuable strategy, particularly for obtaining antibodies directed against epitopes that are conserved in mammals. A generic procedure is established for the humanization of chicken-derived antibodies. To this end, high-affinity binders of the epidermal growth factor receptor extracellular domain are isolated from immunized chickens using yeast surface display. Complementarity determining regions (CDRs) of two high-affinity binders are grafted onto a human acceptor framework. Simultaneously, Vernier zone residues, responsible for spatial CDR arrangement, are partially randomized. A yeast surface display library comprising  $\approx 300\,000$  variants is screened for high-affinity binders in the scFv and Fab formats. Next-generation sequencing discloses humanized antibody variants with restored affinity and improved protein characteristics compared to the parental chicken antibodies. Furthermore, the sequencing data give new insights into the importance of antibody format, used during the humanization process. Starting from the antibody repertoire of immunized chickens, this work features an effective and fast high-throughput approach for the generation of multiple humanized antibodies with potential therapeutic relevance.

## 1. Introduction

Monoclonal antibodies have been generated against a wide range of therapeutically relevant human proteins. Since the first therapeutic monoclonal antibody Muromonab was approved in 1985,<sup>[1]</sup> a plethora of advanced scientific and technologic methods have emerged for the generation of monoclonal antibodies. While hybridoma technology has been strikingly successful, the use of numerous display systems for antibody identification, including ribosomal display,<sup>[2]</sup> phage display,<sup>[3]</sup> yeast surface display (YSD),<sup>[4,5]</sup> and mammalian display<sup>[6]</sup> emerged over the years. Most approved therapeutic monoclonal antibodies were generated by conventional immunization of mice, rabbits, or other species belonging to the class of Mammalia.<sup>[7]</sup> However, targeting epitopes of interest remains challenging, due to the close phylogenetic relationship to humans.

To overcome this limitation, chicken immunization enabled an alternative route for targeting conserved epitopes, with potentially new therapeutic relevance.<sup>[8–10]</sup> In fact, several companies and research groups reported the generation of high-affinity monoclonal antibodies against conserved epitopes by immunization of chickens.<sup>[11,12]</sup>


Additionally, chicken-derived monoclonal antibodies offer a scope of advantages compared to conventional antibodies from mice and rats. Due to the natural somatic VDJ recombination in mammals, a subset of oligonucleotides covering the molecular diversity of antibodies is required to generate an immune-repertoire-based display library. In contrast, the 3' and 5' region coding for the framework regions 1 (FR1) and 4 (FR4) in chicken antibodies remains conserved during the mechanism of antibody diversification, known as gene conversion.<sup>[13–15]</sup> This enables the complete coverage and amplification of the V-region coding gene repertoire with a single pair of oligonucleotides. Besides this, the average length of the CDR3 repertoire in chickens includes a significantly higher content of disulfide-linked cysteines, which often results in variants with increased stability and complexity.<sup>[16]</sup> To circumvent the potential disadvantages of immunogenicity, transgenic chickens were generated exhibiting a human germline sequence for VH and VL domains, resulting in human antibodies upon avian immunization.<sup>[9]</sup> Still, the

A. Elter, J. P. Bogen, S. C. Hinz, Dr. D. Fiebig, A. Macarrón Palacios, Prof. H. Kolmar

Institute for Organic Chemistry and Biochemistry  
Technical University of Darmstadt  
Alarich-Weiss-Strasse 4, Darmstadt D-64287, Germany  
E-mail: Harald.Kolmar@TU-Darmstadt.de

A. Elter, S. C. Hinz, Prof. H. Kolmar  
Merck Lab @ Technical University of Darmstadt  
Alarich-Weiss-Strasse 4 Darmstadt D-64287, Germany  
J. P. Bogen, Dr. D. Fiebig, Dr. J. Grzeschik  
Ferring Darmstadt Laboratory, Biologics Technology and Development  
Alarich-Weiss-Strasse 4 Darmstadt D-64287, Germany

Dr. B. Hock  
Ferring International Center S.A.  
Chemin de la Vergognausaz 50 Saint-Prex 1162, Switzerland

 The ORCID identification number(s) for the author(s) of this article can be found under <https://doi.org/10.1002/biot.202000231>

© 2020 The Authors. *Biotechnology Journal* published by Wiley-VCH GmbH. This is an open access article under the terms of the Creative Commons Attribution License, which permits use, distribution and reproduction in any medium, provided the original work is properly cited.

DOI: 10.1002/biot.202000231

usage of those transgenic chickens is expensive and these animals do not cover the fully human antibody germline diversity.<sup>[19]</sup>

In respect of the immunogenicity of non-human antibodies in humans, their therapeutic application requires humanization. Several strategies have been reported to minimize their immunogenicity.<sup>[17–20]</sup> Even though *in silico* methods are described for the humanization of chicken-derived antibodies,<sup>[21]</sup> the most straightforward method of humanization is based on the grafting of the six complementarity-determining regions onto a suitable human antibody acceptor framework.<sup>[22]</sup> The often observed reduction of affinity, caused by unfavorable CDR orientation<sup>[22]</sup> can be restored by the application of rational design approaches via mutating key residues (Vernier residues).<sup>[23]</sup> Vernier residues are framework amino acids close to the CDRs and do not contribute directly to the antigen binding but are responsible for the correct orientation of the CDR loops. The correct selection of Vernier residues is essential for humanization purposes by loop transplantation.<sup>[23]</sup> This time-consuming trial and error approach involves the generation and characterization of numerous variants, which does not always result in successful humanization and thus excludes these antibodies from further development.<sup>[11]</sup>

As an alternative approach, the generation of expanded libraries, based on multiple amino acid substitutions of predicted Vernier positions proved to increase the chance of successful humanization while maintaining parental affinity.<sup>[24–27]</sup> In recent years, yeast display emerged as a platform technology that allows the discrimination between low and high-affinity binders on a single clone basis. Moreover, it provides an advanced eukaryotic protein expression apparatus, resulting in the elimination of misfolded or truncated protein variants before display.<sup>[4]</sup> Yeast surface display in combination with fluorescence-activated cell sorting (FACS) enables the fast identification and selection of highly affine variants under controlled selection conditions<sup>[28]</sup> and in previous publications, our workgroup described the isolation of chicken-derived antibodies using this strategy.<sup>[29–33]</sup> Vernier residue randomization and yeast display library screening were successfully applied by Kim and co-workers to the humanization of a chicken-derived phosphothreonine peptide-specific antibody.<sup>[27]</sup> Nevertheless, this approach required a single yeast clone analysis of 30 clones obtained from FACS screening to identify two candidates with desired binding characteristics.<sup>[27]</sup>

Encouraged by these findings indicating that Vernier residue randomization and high throughput variant screening is a valid humanization strategy, we investigated in this study, whether FACS selection of yeast-displayed humanized antibody variants derived from immunized chickens in combination with next-generation sequencing facilitates the humanization process. We compared single-chain variable fragment (scFv) and antigen-binding fragment (Fab) formats of resulting humanized antibodies and found that our strategy provides access to humanized antibodies possessing superior stability and aggregation properties while retaining parental affinity.

## 2. Results

We recently described a procedure for the isolation of chicken-derived scFvs via yeast surface display and FACS. An exemplary

target was the extracellular domain (ECD) of the epidermal growth factor receptor (EGFR). The most affine scFvs against EGFR-ECD termed E1 and E2 displayed similar affinities in the range  $(6.8–28) \times 10^{-9}$  M but comprised different CDR lengths, different disulfide patterns, and targeted nonoverlapping epitopes on EGFR (Figure S1, Supporting Information).<sup>[29]</sup> Since they differ in multiple structural and functional properties, these scFvs were chosen for subsequent humanization approaches.

### 2.1. Library Construction

For the humanization of E1 and E2, the CDRs of the heavy and light chains were grafted *in silico* onto human germline sequences (Table S1 and Figure S2, Supporting Information). Next, the Vernier residues identified by Nishibori and co-workers were partially randomized,<sup>[23,26]</sup> encoding for the original chicken germline residue or a residue that is commonly found in human germline sequences at the respective structural position (Figure S2, Supporting Information).<sup>[25]</sup> To reduce the number of oligonucleotides needed, partially degenerated codons were utilized. In some instances, it was tolerated that at some positions also nonhuman and nonchicken residues were encoded. In summary, permutations of Vernier residues led to 1024 VH and 288 VL variants, resulting in  $2.94 \times 10^5$  possible chain combinations.

In a multistep PCR process, oligonucleotides were fused to full-length VH and VL genes, and the PCR product was analyzed by Sanger sequencing to confirm the correct assembly of oligonucleotides as well as randomization of Vernier residues (data not shown). Gap repair cloning with the yeast display vector pCT<sup>[5]</sup> resulted in at least  $5 \times 10^8$  individual clones for the E1 or the E2 library, respectively.

Likewise, for the generation of Fab libraries, the full-length VH and VL sequences of both humanized clonotypes were incorporated into the pDest Lambda vector via Golden Gate cloning and transformed into EBY100 yeast cells.<sup>[30,34,35]</sup> A library size of at least  $1 \times 10^9$  for the E1 library and the E2 library was achieved, respectively.

### 2.2. Cell Sorting

All four yeast surface display libraries were screened separately by FACS. Yeast cells displaying an EGFR-binding antibody fragment were identified by using a recombinant human EGFR-Fc fusion protein. The initial selection of each library was performed using  $200 \times 10^{-9}$  M EGFR. The following sorting round was performed using  $50 \times 10^{-9}$  M EGFR aimed at isolating higher affinity variants. Without any exception, two sorting rounds were sufficient for the enrichment of EGFR-binding variants derived from all four libraries (Figure 1; Figure S3, Supporting Information).

### 2.3. Next-Generation Sequencing and Analysis

Plasmid DNA of yeast populations of the initial libraries as well as of the first and second sorting rounds were isolated and amplified utilizing barcode primers indicating clonotype, antibody format, sorting round, and a variable domain (Table S2, Supporting Information). Amplicons were analyzed by Illumina sequencing and

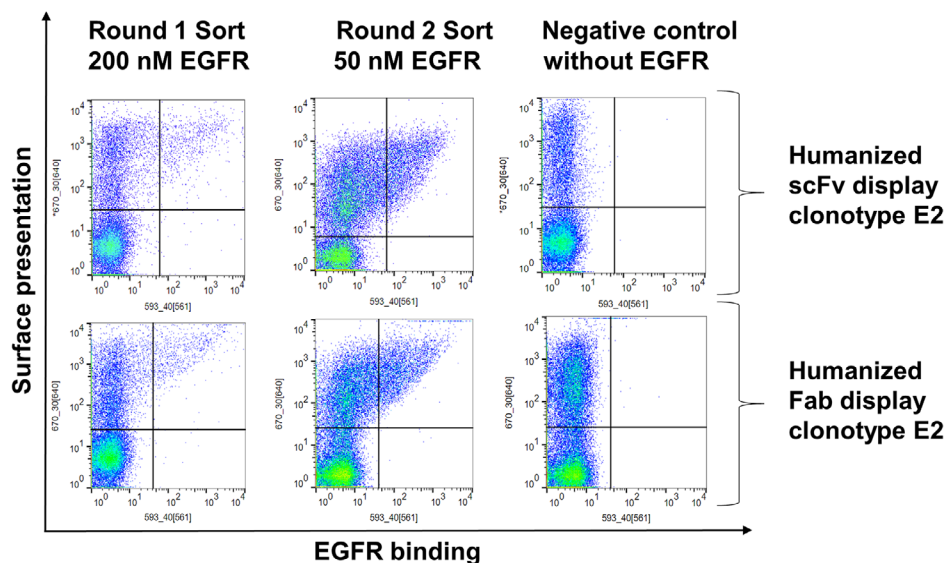


**Figure 1.** YSD Library screening of humanized chicken antibodies of the E2 clonotype. Cells showing both surface presentation (c-myc tag detection for scFvs or antilambda staining for Fabs) and EGFR-Fc binding signal (Fc domain detection) were sorted according to the depicted gating strategy.

the resulting sequences were pairwise aligned and separated by barcodes to enable sequence analysis. Initial libraries contained all possible Vernier residue combinations in VH and VL genes, indicating a full coverage of potential variants.

Sequencing of sorted EGFR binders revealed that not all Vernier residues contributed equally to the antigen-binding properties of humanized antibodies. Throughout sorting, a tryptophan residue at the first Vernier position of the VH sequence of E2-derived humanized antibody variants, which corresponds to the human framework, was found to be significantly enriched, both in Fabs and scFv display constructs (Figure 2A,B,E). Interestingly, the original chicken-derived scFv E2 also exhibits a tryptophan at this position. Humanized VH sequences corresponding to the E1 clonotype showed no enriched occurrence of the tryptophan at the first Vernier position (W47), representing a substantial difference between humanized antibodies derived from E1 and E2 clonotypes (Figure S4; Figure S5, Supporting Information). A significant increase in residue occurrence was also found for alanine at the second Vernier position of VH (A49) for both formats, while the other Vernier residues showed only minor frequency changes, which was true for humanized antibodies corresponding to the E1 and E2 clonotype (Figure 2; Figures S4–S6, Supporting Information). The first Vernier residue of the E1-derived VH sequence showed an increase in leucine frequency upon selection, both in Fabs and scFvs (Figure S6A,B, Supporting Information). In both formats, an enrichment of alanine at the second Vernier position was observed (Figure S6E, Supporting Information). Both clonotypes showed only small residue preferences of single Vernier positions in the VL sequences (Figure 2C,D; Figure S6C,D, Supporting Information).

Furthermore, sequence analysis revealed the enrichment of some Vernier residue combinations after two sorting rounds in comparison with the initial libraries. In the VL sequences, approximately half of all theoretical residue combinations were found after functional variant screening (Figure 2C,D; Figure S6C,D, Supporting Information), while the diversity of residue

combinations was further reduced for the VH enrichment of functional variants and less than 25% of the possible combinations were found (Figure 2A,B; Figure S6A,B, Supporting Information). This indicated the correct orientation of the heavy chain CDRs being more important for antigen binding compared to the light chain CDRs.<sup>[36]</sup> Next, three VH and VL variants of the Fab and three of the scFv library, which showed the strongest enrichment throughout each of the four individual rounds of selection (Tables S3–S6, Supporting Information), were synthesized synthetically.

A combination of respective  $3 \times 3$  VH and VL chains for both variants and both antibody formats resulted in 36 different humanized VH/VL variants (Tables S7–S10, Supporting Information). Additionally, for each clonotype and format, sequences with only human Vernier residues were synthesized, corresponding to a simple CDR grafting approach (Table S11, Supporting Information). Overall, a total number of 40 humanized chicken-mAbs were reformatted and expressed for further characterization. Also, for comparison chicken-derived E1 and E2 were subcloned into a full-length antibody format corresponding to a chimeric IgG (Table S12, Supporting Information).

#### 2.4. Reformating and Expression of Humanized Chicken mAbs

Gene strings were used as templates for amplification, incorporating *SapI* sites for subsequent Golden Gate cloning into a pTT5-derived destination vector utilizing CH1–CH2–CH3 or Lambda-CL entry vectors, respectively.<sup>[32]</sup> To reformat scFvs, amplicons of VH and VL genes were fused into a single chain format and subsequently inserted into a pTT5-derived vector modified into a CH2–CH3 entry vector as described. Primers can be found in Table S12 in the Supporting Information.

Expi293F cells were transiently transfected and after 5 days of cell growth, sterile filtrated supernatant was either directly used for Bio-layer interferometry (BLI) measurements or purified via

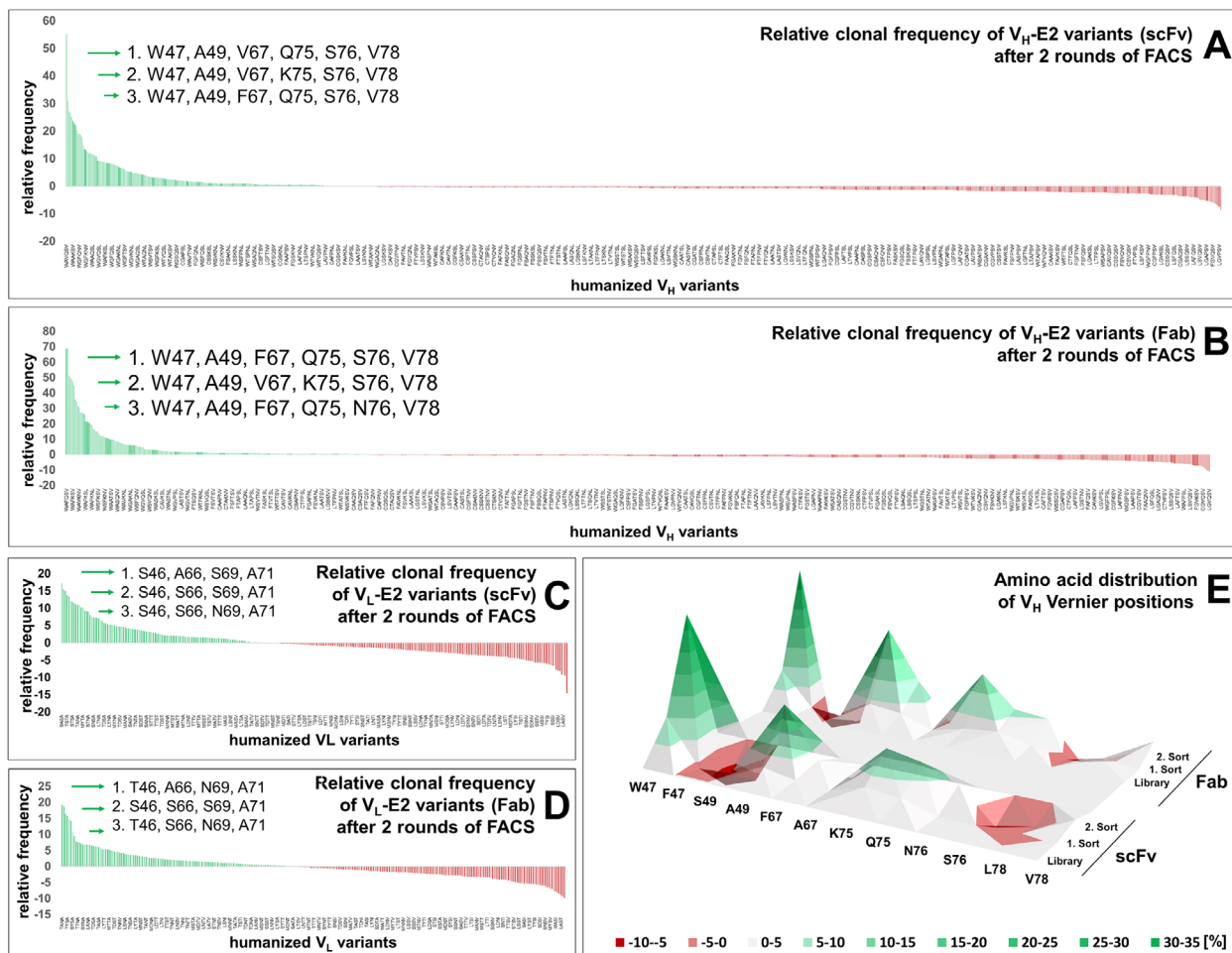


**Figure 2.** Relative enrichment of Vernier position combinations throughout sorting. Next-generation sequencing analysis of humanized clones corresponding to clonotype E2. Clonal frequencies, after two FACS rounds of  $V_H$ -E2 variants corresponding to antibody formats scFv A) and Fab B), relative to the respective clonal frequencies of the initial library sequencing. Clonal frequencies, after two FACS rounds of  $V_L$ -E2 variants corresponding to C) scFv and D) Fabs, relative to the respective clonal frequencies of the initial library sequencing. Most frequent humanized  $V_H$  and  $V_L$  variants (represented by their different Vernier position amino acids) are highlighted by green arrows. E) Analysis of amino acid distribution corresponding to  $V_H$  Vernier positions. Sort-subordinated enriched (green) or decreased (red) proportions (%) of human- and chicken-germline amino acids on Vernier positions, normalized to their respective initial library abundancies.

Protein A affinity chromatography. All variants were successfully produced in the range of 20–30 mg L<sup>-1</sup>. Only the full-length construct of the grafted E1 Fab (gF-E1) (Table S11, Supporting Information), where all Vernier residues originated from the human germline, could not be expressed, underlining the importance of the correct selection of Vernier residue combinations.

## 2.5. Protein Characterization

Binding kinetics for all 36 humanized antibodies (clonotypes E1 and E2, 9 Fabs, and 9 scFvs each) were evaluated by BLI. All variants of clonotype E1 showed single to low double-digit nanomolar equilibrium dissociation constants ( $K_D$ ), while variants of clonotype E2 revealed a broad range between single-digit nanomolar to even triple-digit nanomolar  $K_D$  values (Figures S7–S10, Supporting Information). The most affine variants were purified via Protein A chromatography with subsequent analysis by SDS PAGE

(Figure S11, Supporting Information). The repeated evaluation of binding kinetics using the purified protein samples revealed similar  $K_D$  values compared to measurements using cell culture supernatant. Compared to the parental chicken-derived antibody, similar  $K_D$  values were achieved in humanized variants, ranging from 1.1- to 2.4-fold altered affinity for the E1 clonotype or 0.5–4.6-fold for the E2 clonotype, respectively (Table 1). Additionally, grafted variants of E1 and E2 (gS-E1 and gS-E2) showed a significantly impaired binding to EGFR compared to the parental chicken antibody, the humanized antibodies, and scFv–Fc molecules (hF8-E1, hF1-E2, hS7-E1, and hS9-E2) in BLI analysis, underscoring the importance of Vernier residue optimization (Figure S12A–D, Supporting Information).

Humanized scFv–Fc fusions and humanized full-length antibodies were further examined regarding their thermal stability utilizing DSF and aggregation behavior using HPLC-SEC in native conditions. Full-length antibodies hF8-E1 and hF9-E1 showed favorable melting temperatures of 72.3 and 69.3 °C,

**Table 1.** Binding kinetics and thermal stabilities of humanized scFv–Fc and full-length antibodies compared to parental chicken scFv–Fc molecules (cS-E1 and cS-E2).<sup>[29]</sup> Standard error determination of kinetic parameters was calculated using ForteBio data analysis software 9.0 incorporating at least four different antigen concentrations..

Clonotype E1	$K_D$ [ $\times 10^{-9}$ M]	$K_{on}$ [ $M^{-1} s^{-1}$ ]	$K_{dis}$ [ $s^{-1}$ ]	$K_D$ factor	$K_{on}$ factor	$K_{dis}$ factor	$T_M$ [ $^{\circ}C$ ]
hF8-E1	7.6 $\pm 0.1$	$1.08 \times 10^5$ $\pm 6.8 \times 10^2$	$8.19 \times 10^{-4}$ $\pm 3.7 \times 10^{-6}$	1.1	0.32	2.81	72.3
hF9-E1	9.6 $\pm 0.1$	$1.18 \times 10^5$ $\pm 3.2 \times 10^2$	$1.13 \times 10^{-3}$ $\pm 1.8 \times 10^{-6}$	1.4	0.35	2.04	69.3
hS6-E1	16.1 $\pm 0.1$	$1.1 \times 10^5$ $\pm 1.1 \times 10^3$	$1.76 \times 10^{-3}$ $\pm 4.6 \times 10^{-6}$	2.4	0.32	1.31	54.6
hS7-E1	9.7 $\pm 0.1$	$1.37 \times 10^5$ $\pm 4.4 \times 10^2$	$1.33 \times 10^{-3}$ $\pm 2.2 \times 10^{-6}$	1.4	0.4	1.73	60.0
cS-E1	6.8 $\pm 0.1$	$3.4 \times 10^5$ $\pm 1.6 \times 10^3$	$2.3 \times 10^{-3}$ $\pm 6 \times 10^{-6}$	1	1	1	57.2

Clonotype E2	$K_D$ [ $\times 10^{-9}$ M]	$K_{on}$ [ $M^{-1} s^{-1}$ ]	$K_{dis}$ [ $s^{-1}$ ]	$K_D$ factor	$K_{on}$ factor	$K_{dis}$ factor	$T_M$ [ $^{\circ}C$ ]
hF1-E2	33.5 $\pm 0.7$	$1.97 \times 10^5$ $\pm 4.1 \times 10^3$	$6.58 \times 10^{-3}$ $\pm 4.7 \times 10^{-5}$	1.2	0.66	1.32	71.0
hF8-E2	12.9 $\pm 0.3$	$1.96 \times 10^5$ $\pm 3.7 \times 10^3$	$2.54 \times 10^{-3}$ $\pm 2.2 \times 10^{-5}$	0.5	0.65	3.43	67.8
hS2-E2	128 $\pm 2.7$	$1.23 \times 10^5$ $\pm 1.6 \times 10^3$	$1.69 \times 10^{-2}$ $\pm 6.6 \times 10^{-5}$	4.6	0.41	0.51	51.1
hS9-E2	37.1 $\pm 0.9$	$2.08 \times 10^5$ $\pm 3.9 \times 10^3$	$7.72 \times 10^{-3}$ $\pm 4.6 \times 10^{-5}$	1.3	0.69	1.13	54.5
cS-E2	28 $\pm 0.3$	$3.00 \times 10^5$ $\pm 7.5 \times 10^3$	$8.7 \times 10^{-3}$ $\pm 2.1 \times 10^{-5}$	1	1	1	53.9

Protein characteristics of chicken scFv–Fc molecules cS-E1 and cS-E2 (red) and humanized full-length antibodies and scFv–Fc molecules (green).  $K_D$  factor =  $K_D$  (humanized clone) /  $K_D$  (parental chicken clone) ·  $K_{on}$  factor =  $K_{on}$  (humanized clone) /  $K_{on}$  (parental chicken clone) ·  $K_{dis}$  factor =  $K_{dis}$  (parental chicken clone) /  $K_{dis}$  (humanized clone) ·

respectively, while the humanized scFv variants hS6-E1 and hS7-E1 revealed typical melting temperatures of 54.6 and 60 °C, which is in accordance to melting temperatures reported for human and humanized scFvs<sup>[37,38]</sup> (Table 1; Figure S13, Supporting Information). In the case of the humanized full-length antibodies and scFv–Fc fusions belonging to clonotype E2, thermal stability determination revealed generally lower melting temperatures, probably resulting from the thermal stability of the parental chicken scFv E2.<sup>[37,38]</sup> SEC protein aggregation measurements of the humanized full-length antibodies hF8-E1 and hF9-E1 revealed 0.0% and 2.98% aggregates, respectively, indicating superior properties compared to the parental antibody (Figure 3A; Figure S14A,B, Supporting Information). Surprisingly, the full-length antibodies hF1-E2 and hF8-E2 exhibited 25.23% and 44.29% of multimers, whereas the scFv–Fc constructs hS2-E2 and hS9-E2 with 93.15% and 96.45% of the monomeric fraction were superior compared to the parental chicken scFv–Fc protein (Figure S14C, Supporting Information). Additionally, it was investigated, whether the humanized antibody candidates (hF8-E1, hS7-E1, hF1-E2, and hS9-E2) and the parental chicken antibodies (cS-E1 and cS-E2) demonstrate binding to EGFR-positive A431 cells (Figure 3B). All antibodies bound to A431 cells in a concentration-dependent manner, while all humanized antibody variants demonstrated cell binding comparable to the respective chicken antibody. Calculated EC50

values of humanized antibody variants hF1-E2 and hS9-E2 were in the same range as the EC50 value of the chicken antibody cS-E2. While hS7-E1 demonstrated a similar EC50 value related to the parental chicken antibody cS-E1, hF8-E2 showed slightly impaired binding to EGFR positive A431 cells (Figure 3B). Comparing the protein characteristics of our humanized antibody variants we identified two lead candidates (hF8-E1 and hS9-E2), possessing restored affinity, elevated thermal stability, and improved aggregation behavior compared to the parental chicken antibody (Figure 3 and Table 1; Figure S14, Supporting Information).

### 3. Discussion

In this work, we aimed at establishing a humanization strategy for chicken-derived antibodies by a combination of yeast surface display and next-generation sequencing. It starts from CDR grafting onto a human germline framework and is based on the randomization of Vernier residues, key residues for CDR orientation. Exemplarily, the CDRs of two chicken-derived scFvs were grafted onto a human acceptor framework. Simultaneous randomization of 10 Vernier residues in the VH and VL domains resulted in yeast libraries expressing humanized scFv and Fab fragments. Via YSD and FACS, high affine antibodies

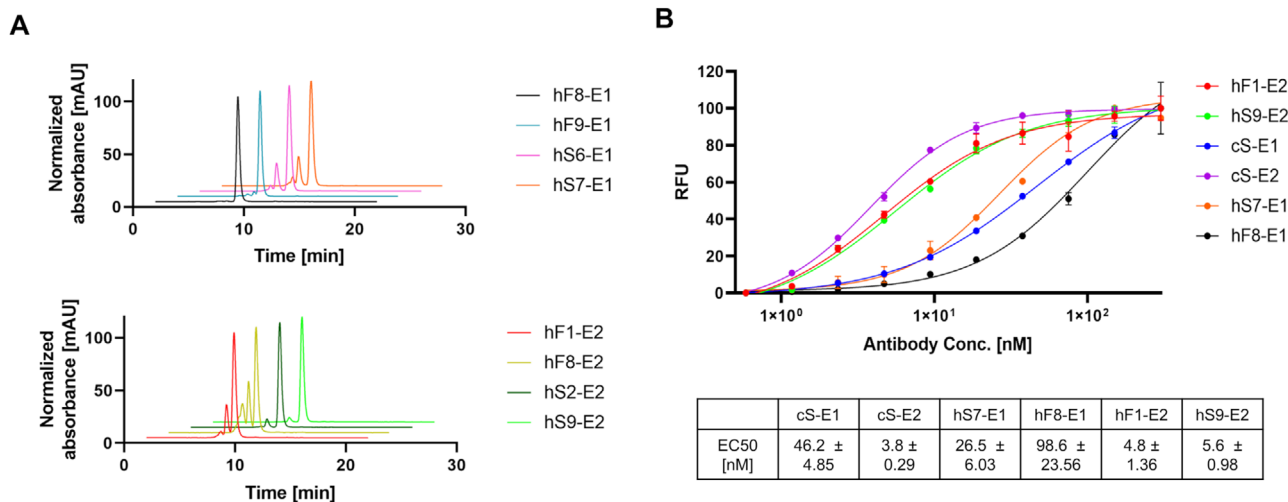


**Figure 3.** A) Determination of protein aggregation behavior by size exclusion chromatography of humanized variants hF8-E1, hF9-E1, hS6-E1, hS7-E1, hF1-E2, hF8-E2, hS2-E2, and hS9-E2. B) Flow-cytometric analysis of A-431 cells using the humanized full-length antibodies hF1-E2, hS9-E2, hS7-E1, hF8-E1, and the chicken-derived antibodies cS-E1 and cS-E2. EC50 values and standard deviations were calculated using data from experimental triplicates.

were isolated, and the sequences were verified by NGS. It was observed that the Vernier residues enriched after two sorting rounds correlate between both antibody formats (Figure 2A,B; Figure S6A,B, Supporting Information). A similar strategy was applied by Nishibori et al. using a phage display strategy. For this type of humanization strategy, the known feature of yeast surface display selection to discriminate between low and high-affinity binders allows for the fast enrichment of sequences encoding functional antibody fragments. Phage display screening required seven rounds of panning and phage amplification,<sup>[26]</sup> while YSD required only two screening rounds to enrich high-affinity binders. While in previous work by Nishibori et al. the “most humanized” antibodies from their phage display campaign after panning were selected,<sup>[26]</sup> we identified variants that showed the strongest enrichment within two rounds of sorting by NGS. Due to FACS-assisted sorting, a more stringent selection could be performed and the number of screening rounds was significantly reduced, resulting in a fast and convenient humanization process. Furthermore, we investigated the possibility to transform scFv molecules into full-length antibodies during humanization. This combines the fast library generation and screening process of single-chain antibodies<sup>[31]</sup> with the foreseen beneficial properties of full-length mAbs.<sup>[39]</sup>

While aiming at reducing immunogenicity, the main issue in humanization campaigns is to restore the properties of the parental antibody. Our combinatorial approach of shuffling the most frequent VH and VL domains for each format and clonotype resulted in a large variety of antibodies retaining the parental antibody affinity and exhibiting superior biophysical properties. The higher thermal stability of all E1 variants compared to the E2 clonotypes is most probably caused by a predicted disulfide bond within the CDR-H3. Additional disulfide bonds are often observed within chicken-derived antibodies and can be used to engineer other semisynthetic scaffolds facilitating higher stability and complexity of CDRs and binding loops.<sup>[16,40,41]</sup>

The utilized human acceptor framework VH3-23 (DP-47) is one of the most frequently found in vivo<sup>[42]</sup> and is also fre-

quently used for therapeutic antibodies, underlining its favorable biophysical properties.<sup>[43]</sup> Since the tendency toward aggregation was mostly found in E2-derived full-length antibodies, we assume this was due to switching of the antibody format.

Except for gF-E1, all grafted variants were producible in ExpiHEK293F cells but failed to show specific binding of EGFR. These results underline the importance of the correct choice of Vernier residues to facilitate expression and high-affinity binding. Even though NGS analysis revealed no major differences in Vernier residue frequency between scFvs and Fabs, there were significant differences between E1 and E2, predominantly at position 47 of the VH. While E2 showed an enrichment of the human-like residue tryptophan at that position, in E1 the non-human/non-chicken residue leucine was more frequently present. Since it is not predictable which residue facilitates favorable binding behavior, a library based-approach as performed in this study is mandatory for the humanization of chicken-derived antibodies.

We analyzed the sequences of humanized antibodies that were approved in the United States between 2018 and March 2020 and compared their germline identity with the germline identity of our humanized variants (Table S13, Supporting Information). For the approved mAbs, the identity of the VH sequences to their respective germlines ranged between 76.5% and 87.8%. The humanized chicken-derived antibodies presented in this study ranged between 83.7% and 85.7% and are therefore on average at least as close to the human germline as approved antibodies. VL sequences of approved mAbs ranged between 80.0% and 92.9% identity to their respective germline. The humanized E1 and E2 VL sequences resulted in a comparable range between 77.1% and 80.9% identity. In respect to the overall germline identity of the Fv fragments, chicken-derived antibodies humanized in this study (80.9–82.8%) are as close to the human germline as approved humanized antibodies (79.7–85.5%).

To gain deeper insights into the potential immunogenicity of the humanized E1 and E2 variants, we analyzed peptides derived from the Fv fragments for their binding ability toward MHCII in

silico (Table S13, Supporting Information). We found 4 strong MHCII binding peptides in all VH domains, which was very similar to what we found in approved humanized antibodies. In respect to weak binding peptides, the calculated number of peptides ranged from 8 to 16 in humanized chicken mAbs and 6 to 15 in approved antibodies. While the VL domains exhibited no strong MHCII binding peptides, the approved antibodies comprised up to 5 strongly immunogenic peptides. Between 7 and 9 weak MHCII binding peptides were found in the VL of humanized chicken mAbs from this work, while approved antibodies exhibited 4 to 22. This underlines the suitability of our approach for the humanization of avian-derived antibodies.

An alternative approach for chicken antibody humanization was recently described by Symphogen using a strategy termed “mass complementarity-determining region grafting.”<sup>[11]</sup> Here, several dozens of promising chicken antibodies were individually humanized via CDR grafting on several human frameworks followed by in silico modeling and generation of up to four Vernier variants for each clonotype. With this approach, a significant fraction of clonotypes was lost, when none of the Vernier variants displayed target affinity.<sup>[11]</sup> While this approach is partially based on the alteration of a single Vernier position, located in the VH framework region 3, we identified 2 Vernier positions (VR49 for E1 and VR47 and VR49 for E2) within the VH framework region 2, which showed the strongest enrichment of certain amino acids after two rounds of cell sorting and analysis via NGS resulting in the successful humanization of both chicken antibodies. Since we used a simple Golden Gate cloning strategy for library generation and inexpensive degenerated primers for Vernier residue randomization, simultaneous humanization of a larger set of clonotypes could be envisioned. With approximately 300 000 Vernier combinations of each clonotype, the library diversity is relatively small compared to the screening capacities of a high throughput FACS device. Hence, it might be feasible to combine randomized candidates of several clonotypes for simultaneous two-round-FACS screening followed by NGS analysis, thereby potentially enhancing the hit rate and hit quality of a whole binder set.

Since all chicken-derived antibodies originate from a limited pool of homologous pseudogenes, the presented method is most probably suitable for the humanization of almost all chicken-derived antibodies. Currently, a large set of chicken-derived antibodies, humanized with the described method are under investigation by our group.

Taken together, we demonstrated a fast and easy approach to transform chicken-derived scFvs into humanized scFv–Fc fusions and full-length antibodies, exhibiting superior properties compared to the parental variant while being as human as state-of-the-art humanized approved antibodies. This further eases the path to utilize avian immunization for the development of humanized chicken-derived antibodies for therapeutic applications.

## 4. Experimental Section

**Plasmids:** For the display of scFv molecules on yeast cells the pCT vector was used.<sup>[5]</sup> It encodes an ampicillin resistance gene and a tryptophan auxotrophic marker, as well as a *GAL1* promoter, *Aga2p* expression sequence, and the respective scFv gene. For the display of Fab fragments,

the pDest Lambda vector, as well as the entry vector of Rosowski et al. was utilized.<sup>[34,35]</sup> The entry vector carries a kanamycin resistance, and a *GAL1, 10* promoter, flanked by *BsaI* sites. The destination vector carries an ampicillin resistance, a tryptophan auxotrophic marker, a human Lambda-CL, a stuffer sequence flanked by *BsaI* sites, a human CH1 domain, as well as the *Aga2p* expression sequence.

For soluble expression of mAbs, a pTT5-derived vector (Expresso CMV-based system, Lucigen), was utilized carrying ampicillin resistance. It was used as a destination vector carrying *SapI* sites for Golden Gate cloning. As entry vectors, pYD-derived plasmids carrying a kanamycin resistance were utilized. For the reformatting of heavy chains, an entry vector comprising the CH1–CH2–CH3 sequences were used. For the expression of light chains, a precloned Lambda-CL comprising entry vector was utilized while scFvs were reformatted with a CH2–CH3 entry vector.<sup>[32]</sup>

**Library Design and Library Generation:** CDR-H1-3 of both chicken-derived scFv variants E1 and E2 were grafted in silico onto human germline acceptor frameworks IGHV3-23 and JH4, whereas the CDR-L1-3 were grafted onto the human germlines IGLV3-25 and JL2.<sup>[26]</sup> In accordance, the Vernier residues of the heavy chain (H47, 49, 67, 75, 76, and 78) and the light chain (L46, 66, 69, and 71) were partially randomized using oligonucleotides containing degenerated codons.<sup>[26]</sup> Oligonucleotides were ordered at Sigma-Aldrich (Table S1, Supporting Information). In a three-step PCR process, oligonucleotides were fused resulting in full-length humanized VH and VL genes of both clonotypes, exhibiting overhangs for Golden Gate cloning via *BsaI* and were used for subcloning as described.<sup>[34,35]</sup>

In an additional fourth PCR reaction, VH and VL genes were fused into an scFv format encoding a (G<sub>4</sub>S)<sub>3</sub> linker and containing terminal overhangs homologous to the pCT vector for gap repair in yeast as described previously.<sup>[5,29]</sup> All PCR reactions were performed utilizing Q5 polymerase (New England Biolabs) according to the manufacturer's protocol and were purified via the Wizard SV Gel and PCR Clean-up System (Promega). Each yeast surface display library was generated separately according to Benaït et al.<sup>[44]</sup>

**Yeast Strains and Media:** For yeast surface display library generation *Saccharomyces cerevisiae* strain EBY100 [MATa URA3-52 trp1 leu2Δ1 his3Δ200 pep4:HIS3 prb1Δ1.6R can1 GAL (pIU211:URA3)] (Thermo Fisher Scientific) was utilized. Cultivation was performed in a YPD medium composed of 20 g L<sup>-1</sup> peptone/casein, 20 g L<sup>-1</sup> glucose, and 10 g L<sup>-1</sup> yeast extract. After library generation, yeast cells were cultivated in SD-CAA media comprised of 5.4 g L<sup>-1</sup> Na<sub>2</sub>HPO<sub>4</sub> and 8.6 g L<sup>-1</sup> NaH<sub>2</sub>PO<sub>4</sub> × H<sub>2</sub>O, 20 g L<sup>-1</sup> glucose, 5 g L<sup>-1</sup> ammonium sulfate, 1.7 g L<sup>-1</sup> yeast nitrogen base (without amino acids), and 5 g L<sup>-1</sup> bacto casamino acids. For induction of scFv or Fab display, cells were transferred into SG-CAA media, containing galactose instead of glucose and incubated at 30 °C, 180 rpm overnight. Yeast cell cultivation using agar plates was performed with SD-CAA medium supplemented with 7% agar-agar.

**Cell Sorting and Flow Cytometry:** Before each cell sorting, yeast cells were cultivated overnight in an SD-CAA medium. Cells were transferred to the SG-CAA medium, at an initial cell density of approximately 1 × 10<sup>7</sup> cells mL<sup>-1</sup>. To ensure sufficient display levels, cells were incubated at least for 12 h. All incubation steps were performed at 180 rpm and 30 °C. Yeast cells were separated by centrifugation and washed with 1 mL of PBS (pH 7.4) containing 0.1% (w/v) bovine serum albumin (BSA) (5 × 10<sup>7</sup> cells mL<sup>-1</sup> PBS) before proceeding with the immunostaining procedure (1 × 10<sup>7</sup> cells/20 μL). The surface display of assembled Fab molecules was detected using the antihuman lambda Alexa Flour 647 (AF647)-conjugated antibody (SouthernBiotech). The validation of scFv display was enabled by using anti-c-myc biotin antibody (Miltenyi Biotec) and streptavidin–allophycocyanin (APC) (Fisher Scientific). EGFR-Fc (R&D Systems) served as the antigen. To detect EGFR binding goat antihuman IgG Fc secondary antibody PE (Invitrogen) was utilized. Cell sorting and flow cytometric analysis were performed using the BD Influx cell sorter and the BD FACS software 1.0.0.650. Sorted yeast cells were transferred onto SD-CAA agar plates and incubated for at least 48 h. Concerning the maintenance of diversity, in the subsequent sorting round at least 50–100-fold the number of sorted cells of the prior round was screened. To determine the ability of the humanized and parental chicken antibodies to bind EGFR-positive cells, A431 cells were trypsinized and washed with PBS (pH 7.4) containing

0.1% (w/v) BSA before proceeding with the immunostaining procedure.  $2 \times 10^7$  cells were incubated for 30 min in 100  $\mu$ L of the respective antibody solution. Cells were washed two times with 200  $\mu$ L PBS (pH 7.4) 0.1% (w/v) BSA, followed by 30 min incubation in 50  $\mu$ L PBS (pH 7.4) 0.1% (w/v) BSA containing 1  $\mu$ g goat antihuman IgG Fc secondary antibody PE (Invitrogen). After two additional wash steps with 200  $\mu$ L PBS (pH 7.4) 0.1% (w/v) BSA cells were analyzed using the BD Influx cell sorter and the BD FACS software 1.0.0.650.

**Next-Generation Sequencing and Sequence Analysis:** Yeast cell populations of the initial libraries as well as of the first and second sorting rounds were cultivated in SD-CAA media and harvested after overnight incubation at 30 °C at 180 rpm. Plasmids were isolated utilizing the Zymoprep Yeast Plasmid Miniprep kit (Zymo Research). VH and VL genes were amplified separately for each library and sorting round using barcode primers (Table S2, Supporting Information). Amplicons were purified from an agarose gel and used as a template for a second PCR reaction utilizing the same primer pairs. PCR reactions were performed utilizing Q5 polymerase (New England Biolabs) according to the manufacturer's protocol and purified using the Wizard SV Gel and PCR Clean-up System. For next-generation sequencing, the VH and VL amplicons of each clonotype were sent to Genewiz for Illumina sequencing. The resulting sequences were analyzed using Geneious Prime 2019.0.4.

**Reformatting, Expression, and Purification of Antibodies:** VH and VL genes were ordered as gene strings from Twist Bioscience. For reformatting as full-length antibodies, VH and VL genes were amplified utilizing primers incorporating terminal *SapI* sites for Golden Gate cloning. Amplicons were inserted into a pTT5-derived vector utilizing the CH1-CH2-CH3 or lambda entry vectors,<sup>[32]</sup> respectively, according to the manufacturer's protocol. PCR reactions were performed utilizing Q5 polymerase (New England Biolabs) according to the manufacturer's protocol and purified using the Wizard SV Gel and PCR Clean-up System (Promega). For scFvs, the VH and VL genes were amplified incorporating terminal overhangs and *SapI* sites, respectively. Via overlap extension PCR, amplicons were fused into an scFv format and subcloned into a pTT5-derived vector utilizing the CH2-CH3 entry vector according to the manufacturer's protocol.

*Escherichia coli* DH5 $\alpha$  were transformed utilizing the Golden Gate reaction mixtures and were cultivated on ampicillin dYT agar plates (10 g L<sup>-1</sup> tryptone, 5 g L<sup>-1</sup> yeast extract, 10 g L<sup>-1</sup> NaCl, and 10 g L<sup>-1</sup> agar-agar). Resulting colonies were directly sequenced at MicroSynth SeqLab, and positive clones were utilized to inoculate 50 mL overnight cultures. Plasmid DNA was isolated using the Promega PureYield Plasmid Midiprep System and used for transient transfection.

Expi293F cells were cultivated in 30 mL Expi293 Expression Medium (ThermoFisher) for two days at 37 °C and 8.0% CO<sub>2</sub> at 110 rpm. Transient transfection was performed utilizing Transporter 5 polyethyleneimine (PEI) according to the manufacturer's protocol (Polyscience). After 5 days, cell culture supernatants were sterile filtrated and either directly used for the determination of binding kinetics or further purified. Purification was performed using an ÄKTA Pure 25L FPLC system with HiTrap Protein A HP columns (GE Healthcare) according to the manufacturer's protocol. Subsequently, buffer exchange against PBS (pH 7.4) was performed utilizing HiTrap Desalting columns (GE Healthcare).

**Biolayer Interferometry:** Before protein purification and further characterization, biolayer interferometry was used to identify most affine humanized scFv-Fc and full-length antibody variants. The Octet RED96 system (FortéBio, Molecular Devices) was utilized. Antihuman IgG Fc capture (AHC) biosensors were soaked in PBS (pH 7.4) for at least 10 min before capturing the humanized antibody variants from the cell culture supernatant. Quenching and dissociation steps were performed using Kinetics buffer (FortéBio) diluted 1:10 in PBS (pH 7.4). EGFR-ECD (produced in house) concentrations ranged from  $3.75 \times 10^{-9}$  to  $960 \times 10^{-9}$  M, depending on the antibodies' clonotype (E1/E2). For each experiment, a negative control was performed using kinetics buffer instead of the antigen-containing solution. Data analysis was performed with FortéBio data analysis software 9.0. After subtraction of the respective negative control (using kinetics buffer instead of EGFR), binding kinetics were determined based on Savitzky-Golay filtering and a 1:1 Langmuir binding

model. Binding kinetics of hF8-E1, hF9-E1, hS6-E1, hS7-E1, hF1-E2, hF8-E2, hS2-E2, and hS9-E2 were redetermined using purified protein samples.

**Size Exclusion Chromatography:** Size exclusion chromatography was performed using the Agilent Technologies 1260 Infinity system. 10  $\mu$ g of protein was injected on a TSKgel SuperSW3000 column (Tosoh) applying a constant flow rate of 0.35 mL min<sup>-1</sup> using sterile filtered and degassed PBS (pH 7.4).

**Nanodifferential Scanning Fluorimetry Measurement:** The thermal stability of proteins was evaluated using the Prometheus NT.48 system (Nano-temper Technologies). Prometheus NT.48 capillaries were loaded with 10  $\mu$ L of protein solution (0.4 mg mL<sup>-1</sup> in PBS pH 7.4). Melting temperature was determined by the ratio of the fluorescence's first derivative at 330 and 350 nm during a temperature gradient of 1 °C min<sup>-1</sup> ranging from 20 to 90 °C.

## Supporting Information

Supporting Information is available from the Wiley Online Library or from the author.

## Acknowledgements

A.E. and J.P.B. contributed equally to this work. The authors would like to thank the Merck Lab @ Technical University of Darmstadt and the Ferring Darmstadt Laboratory for funding. The authors also would like to thank Prof. Fessner for the possibility to perform NanoDSF measurements within his laboratory. The authors declare that this study received funding from the Merck Lab at the Technical University of Darmstadt and the Ferring Darmstadt Laboratory. The funders had no role in study design, data collection, and analysis, decision to publish, or preparation of the manuscript.

Open access funding enabled and organized by Projekt DEAL.

## Data Availability Statement

The data that supports the findings of this study are available in the supplementary material of this article.

## Author Contributions

A.E. assisted in conceptualization, data curation, investigation, methodology, project administration, validation; visualization, writing original draft, and writing review and editing. J.P.B. assisted in conceptualization, data curation, investigation, methodology, project administration, validation, visualization, writing original draft, and writing review and editing. S.C.H. assisted in visualization. David Fiebig assisted in methodology and visualization. A.M.P. assisted in methodology. J.G. assisted in supervision. B.H. assisted in supervision. H.K. assisted in supervision, writing original draft, and writing review and editing.

## Conflict of Interest

The authors declare no conflict of interest.

## Keywords

chicken antibody, fluorescence-activated cell sorting, humanization, next-generation sequencing, yeast surface display

Received: May 18, 2020  
Revised: October 6, 2020  
Published online:



- [1] S. L. Smith, *J. Transplant Coord.* **1996**, 6, 109.
- [2] L. C. Mattheakis, R. R. Bhatt, W. J. Dower, *Proc. Natl. Acad. Sci. USA* **1994**, 91, 9022.
- [3] J. McCafferty, A. D. Griffiths, G. Winter, D. J. Chiswell, *Nature* **1990**, 348, 552.
- [4] M. J. Feldhaus, R. W. Siegel, L. K. Opresko, J. R. Coleman, J. M. Feldhaus, Y. A. Yeung, J. R. Cochran, P. Heinzelman, D. Colby, J. Swers, C. Graff, H. S. Wiley, K. D. Wittrup, *Nat. Biotechnol.* **2003**, 21, 163.
- [5] E. T. Boder, K. D. Wittrup, *Nat. Biotechnol.* **1997**, 15, 553.
- [6] M. Ho, I. Pastan, *Methods Mol. Biol.* **2009**, 525, 337.
- [7] R. M. Lu, Y. C. Hwang, I. J. Liu, C. C. Lee, H. Z. Tsai, H. J. Li, H. C. Wu, *J. Biomed. Sci.* **2020**, 27, 1.
- [8] E. L. Davies, J. S. Smith, C. R. Birkett, J. M. Manser, D. V. Anderson-Dea, J. R. Young, *J. Immunol. Methods* **1995**, 186, 125.
- [9] K. H. Ching, E. J. Collarini, Y. N. Abdiche, D. Bedinger, D. Pedersen, S. Izquierdo, R. Harriman, L. Zhu, R. J. Etches, M. C. van de Lavoie, W. D. Harriman, P. A. Leighton, *mAbs* **2018**, 10, 71.
- [10] A. Larsson, R. M. Balow, T. L. Lindahl, P. O. Forsberg, *Poult. Sci.* **1993**, 72, 1807.
- [11] T. Gjetting, M. Gad, C. Frohlich, T. Lindsted, M. C. Melander, V. K. Bhatia, M. M. Grandal, N. Dietrich, F. Uhlenbrock, G. R. Galler, M. Strandh, J. Lantto, T. Bouquin, I. D. Horak, M. Kragh, M. W. Pedersen, K. Koefoed, *mAbs* **2019**, 11, 666.
- [12] J. Andris-Widhopf, C. Rader, P. Steinberger, R. Fuller, C. F. Barbas, 3rd, *J. Immunol. Methods* **2000**, 242, 159.
- [13] N. Maizels, *Annu. Rev. Genet.* **2005**, 39, 23.
- [14] C. A. Reynaud, V. Anquez, J. C. Weill, *Eur. J. Immunol.* **1991**, 21, 2661.
- [15] C. A. Reynaud, A. Dahan, V. Anquez, J. C. Weill, *Cell* **1989**, 59, 171.
- [16] L. Wu, K. Oficjalska, M. Lambert, B. J. Fennell, A. Darmanin-Sheehan, D. Ni Shuilleabhain, B. Autin, E. Cummins, L. Tchistiakova, L. Bloom, J. Paulsen, D. Gill, O. Cunningham, W. J. Finlay, *J. Immunol.* **2012**, 188, 322.
- [17] Y. Safdari, S. Farajnia, M. Asgharzadeh, M. Khalili, *Biotechnol. Genet. Eng. Rev.* **2013**, 29, 175.
- [18] I. I. Singer, D. W. Kawka, J. A. DeMartino, B. L. Daugherty, K. O. Elliston, K. Alves, B. L. Bush, P. M. Cameron, G. C. Cuca, P. Davies, *J. Immunol.* **1993**, 150, 2844.
- [19] M. J. Glennie, P. W. Johnson, *Immunol. Today* **2000**, 21, 403.
- [20] F. A. Harding, M. M. Stickler, J. Razo, R. B. DuBridg, *mAbs* **2010**, 2, 256.
- [21] N. Tsurushita, M. Park, K. Pakabunto, K. Ong, A. Avdalovic, H. Fu, A. Jia, M. Vasquez, S. Kumar, *J. Immunol. Methods* **2004**, 295, 9.
- [22] P. T. Jones, P. H. Dear, J. Foote, M. S. Neuberger, G. Winter, *Nature* **1986**, 321, 522.
- [23] J. Foote, G. Winter, *J. Mol. Biol.* **1992**, 224, 487.
- [24] M. Baca, L. G. Presta, S. J. O'Connor, J. A. Wells, *J. Biol. Chem.* **1997**, 272, 10678.
- [25] M. Dondelinger, P. Filee, E. Sauvage, B. Quinting, S. Muyldermans, M. Galleni, M. S. Vandevenne, *Front. Immunol.* **2018**, 9, 2278.
- [26] N. Nishibori, H. Horiuchi, S. Furusawa, H. Matsuda, *Mol. Immunol.* **2006**, 43, 634.
- [27] D. S. Baek, Y. S. Kim, *Biochem. Biophys. Res. Commun.* **2015**, 463, 414.
- [28] A. Doerner, L. Rhiel, S. Zielonka, H. Kolmar, *FEBS Lett.* **2014**, 588, 278.
- [29] J. Grzeschik, D. Yanakieva, L. Roth, S. Krah, S. C. Hinz, A. Elter, T. Zollmann, G. Schwall, S. Zielonka, H. Kolmar, *Biotechnol. J.* **2019**, 14, 1800466.
- [30] L. Roth, J. Grzeschik, S. C. Hinz, S. Becker, L. Toleikis, M. Busch, H. Kolmar, S. Krah, S. Zielonka, *Biol. Chem.* **2019**, 400, 383.
- [31] J. P. Bogen, J. Grzeschik, S. Krah, S. Zielonka, H. Kolmar, *Methods Mol. Biol.* **2020**, 2070, 289.
- [32] J. P. Bogen, J. Storka, D. Yanakieva, D. Fiebig, J. Grzeschik, B. Hock, H. Kolmar, *Biotechnol. J.* **2020**, 2000240. <https://doi.org/10.1002/biot.202000240>
- [33] S. C. Hinz, A. Elter, O. Rammo, A. Schwämmle, A. Ali, S. Zielonka, T. Herget, H. Kolmar, *Front. Bioeng. Biotechnol.* **2020**, 8, 688.
- [34] S. Rosowski, S. Becker, L. Toleikis, B. Valldorf, J. Grzeschik, D. Demir, I. Willenbuecher, R. Gaa, H. Kolmar, S. Zielonka, S. Krah, *Microb. Cell Fact.* **2018**, 17, 3.
- [35] S. Krah, J. Grzeschik, S. Rosowski, R. Gaa, I. Willenbuecher, D. Demir, L. Toleikis, H. Kolmar, S. Becker, S. Zielonka, *Methods Mol. Biol.* **2018**, 1827, 145.
- [36] S. Krah, C. Schroter, C. Eller, L. Rhiel, N. Rasche, J. Beck, C. Sellmann, R. Gunther, L. Toleikis, B. Hock, H. Kolmar, S. Becker, *Protein Eng., Des. Sel.* **2017**, 30, 291.
- [37] L. Borrás, T. Gunde, J. Tietz, U. Bauer, V. Hulmann-Cottier, J. P. Grimshaw, D. M. Urech, *J. Biol. Chem.* **2010**, 285, 9054.
- [38] E. Garber, S. J. Demarest, *Biochem. Biophys. Res. Commun.* **2007**, 355, 751.
- [39] V. Quintero-Hernandez, V. R. Juarez-Gonzalez, M. Ortiz-Leon, R. Sanchez, L. D. Possani, B. Becerril, *Mol. Immunol.* **2007**, 44, 1307.
- [40] J. C. Almagro, G. Raghunathan, E. Beil, D. J. Janecki, Q. Chen, T. Dinh, A. LaCombe, J. Connor, M. Ware, P. H. Kim, R. V. Swanson, J. Franson, *J. Mol. Recognit.* **2012**, 25, 125.
- [41] A. P. Silverman, A. M. Levin, J. L. Lahti, J. R. Cochran, *J. Mol. Biol.* **2009**, 385, 1064.
- [42] I. M. Tomlinson, G. Walter, J. D. Marks, M. B. Llewelyn, G. Winter, *J. Mol. Biol.* **1992**, 227, 776.
- [43] T. Tiller, I. Schuster, D. Deppe, K. Siegers, R. Strohn, T. Herrmann, M. Berenguer, D. Poujol, J. Stehle, Y. Stark, M. Hessling, D. Daubert, K. Felderer, S. Kaden, J. Kolln, M. Enzelberger, S. Urlinger, *mAbs* **2013**, 5, 445.
- [44] L. Benatuil, J. M. Perez, J. Belk, C. M. Hsieh, *Protein Eng., Des. Sel.* **2010**, 23, 155.